

## Electronic Supplementary Information

### **Environmental performances of hydrochar-derived magnetic carbon composite affected by its carbonaceous precursor**

Xiangdong Zhu, Feng Qian, Yuchen Liu, Shicheng Zhang\*, Jianmin Chen

Shanghai Key Laboratory of Atmospheric Particle Pollution and Prevention (LAP<sup>3</sup>), Department of

Environmental Science and Engineering, Fudan University, Shanghai 200433, China

\* Corresponding author.

Tel/fax: +86-21-65642297;

E-mail address: [zhangsc@fudan.edu.cn](mailto:zhangsc@fudan.edu.cn).

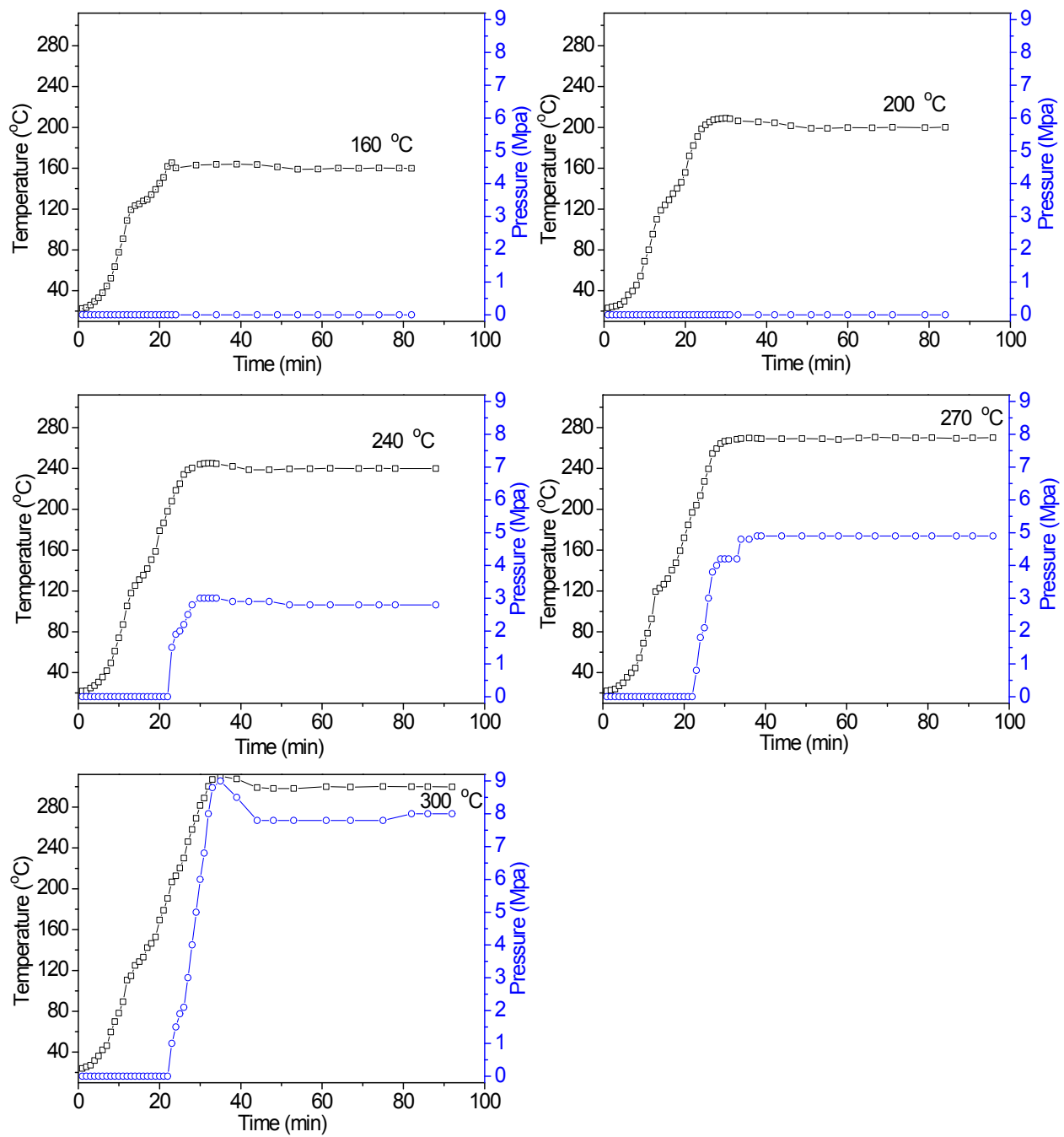


Fig. S1. HTC temperature and pressure variations as a function of reaction time during the HTC process.

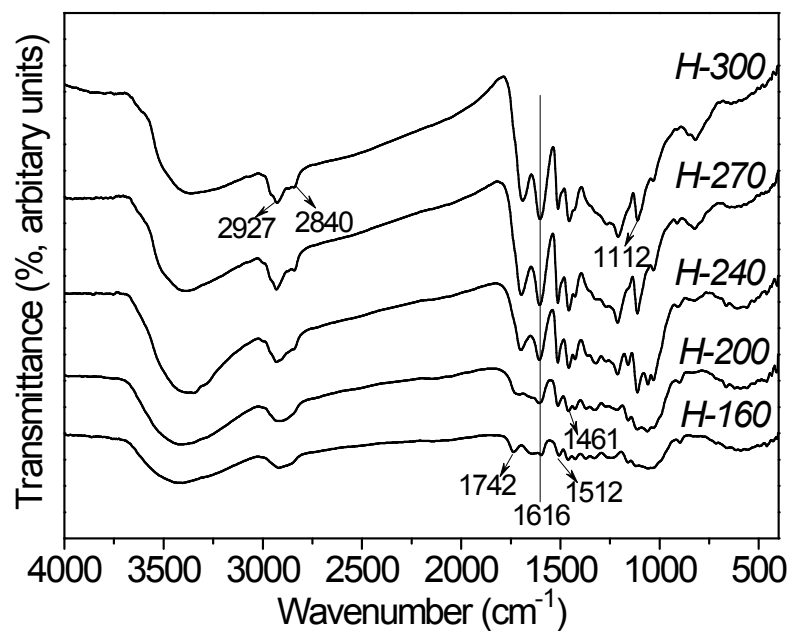


Fig. S2. FTIR spectra for the hydrochar produced at different HTC temperatures.

Abundant FT-IR peaks for hydrochar materials were found, they were similar and different only in the intensity of some peaks, suggesting that the functional group compositions was not greatly changed during the HTC reaction. The aromatic C ( $1616\text{ cm}^{-1}$ ) was observed, and the peak intensity increased with peak temperature of HTC reaction increase, indicating increasing thermal recalcitrance of hydrochar samples. The hydrochar materials also had the adsorption bands at  $2927$  and  $2840\text{ cm}^{-1}$ , which were attributed to stretching vibration of aliphatic C-H. The peak at  $1742\text{ cm}^{-1}$  was assigned to C=O groups, resulted from the acid group (C-OOH). Obviously, the peaks ( $2927$ ,  $2840$  and  $1742\text{ cm}^{-1}$ ) increased with processing HTC reaction, indicating that these aliphatic carbons are mainly produced from the HTC reaction. The band at  $1512\text{ cm}^{-1}$  represented the C=C stretching vibration. The peak at  $1461\text{ cm}^{-1}$  was assigned to C-H deformation vibration. The peak located at  $1112\text{ cm}^{-1}$  was attributed to the C-O stretching vibration.

## Text S1

As shown in Fig. 1b, the DTG curves contained two general regions of weight loss. The first region of weight loss was found from 300 to 350°C, resulting from the thermal oxidation of residual cellulose, hemicellulose and low-boiling products derived from the HTC process. The second region of weight loss was observed above 400°C, due to the thermal oxidation of the more recalcitrant organic substances with the structure of lignin or thermally produced carbonized/aromatic compounds.<sup>1</sup> Obviously, the weight loss of hydrochar samples derived from higher HTC temperatures were focused toward much higher temperatures. Such differences indicated that hydrochar samples produced at higher peak temperatures would be more recalcitrant, which was consistent with the qualitative assessment of  $R_{50}$  for those hydrochar samples.

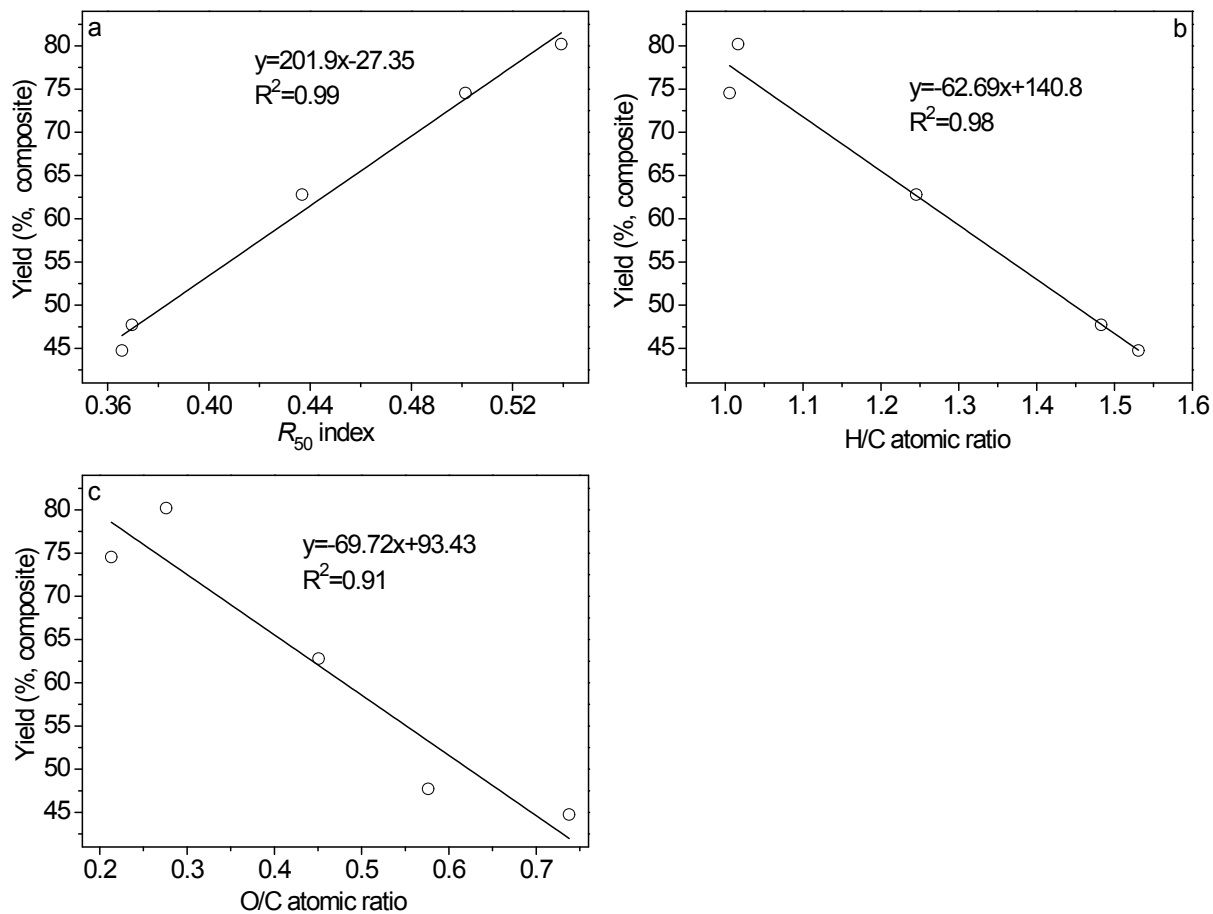


Fig. S3. Correlations between the yields of magnetic carbon composites and the properties of hydrochar precursors:  $R_{50}$  index (a), H/C (b) and O/C (c) atomic ratios.

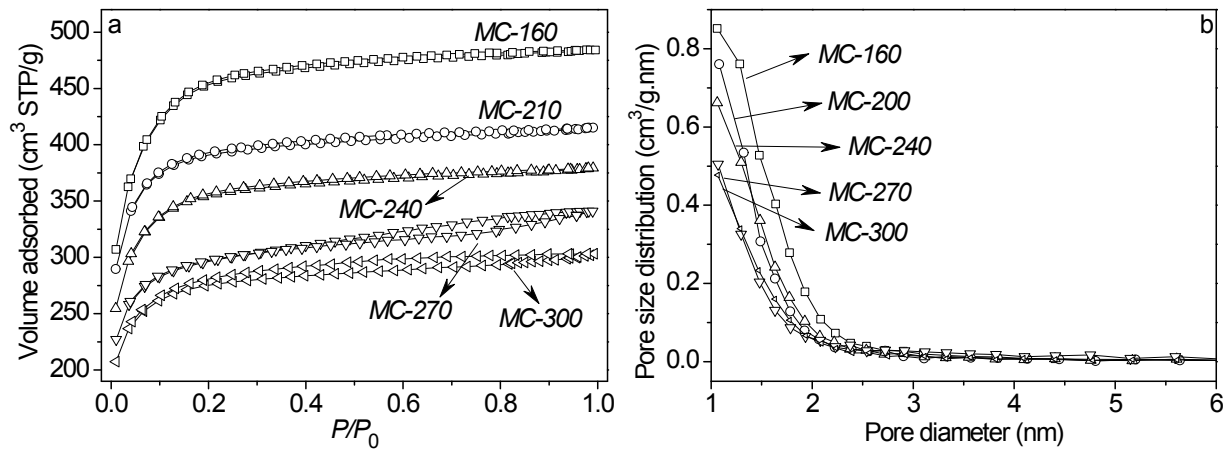


Fig. S4. Nitrogen adsorption isotherms and pore size distribution for the different hydrochar-derived magnetic carbon composites.

Table S1. Regression equation and correlation coefficient of the porosity of magnetic carbon composite related to the properties of hydrochar

Hydrochar Properties	Regression Equation	R <sup>2</sup>
<i>R</i> <sub>50</sub>	BET Surface Area = $-2862R_{50} + 2403$	0.89
	Micropore Surface Area = $-2951R_{50} + 2367$	0.89
	Total Pore Volume = $-1.30R_{50} + 1.17$	0.88
	Micropore Volume = $-1.44R_{50} + 1.16$	0.91
H/C	BET Surface Area = $901H/C + 4.53$	0.90
	Micropore Surface Area = $944H/C - 125$	0.93
	Total Pore Volume = $0.406H/C + 0.0855$	0.87
	Micropore Volume = $0.460H/C - 0.0548$	0.95
O/C	BET Surface Area = $1066O/C + 656$	0.95
	Micropore Surface Area = $1118O/C + 557$	0.98
	Total Pore Volume = $0.476O/C + 0.380$	0.90
	Micropore Volume = $0.541O/C + 0.279$	0.99

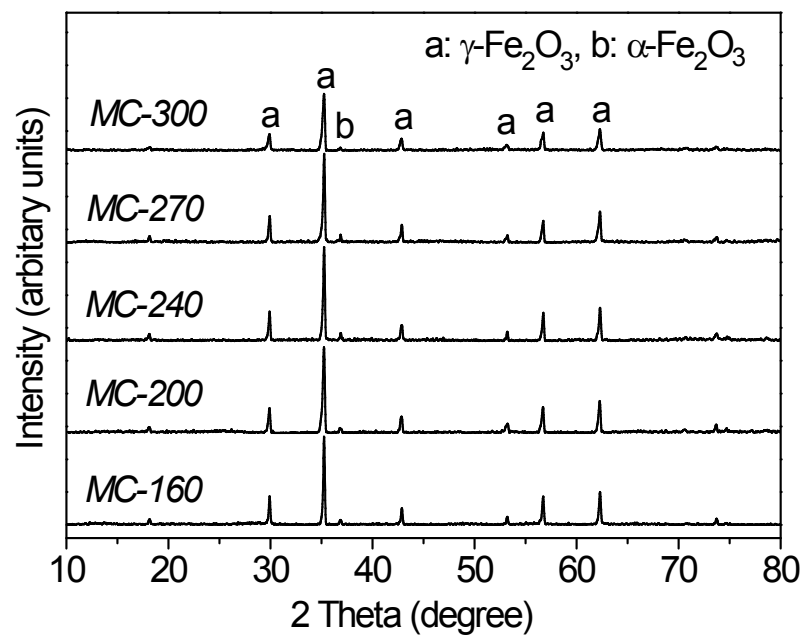


Fig. S5. XRD patterns of the as-prepared magnetic carbon composites.

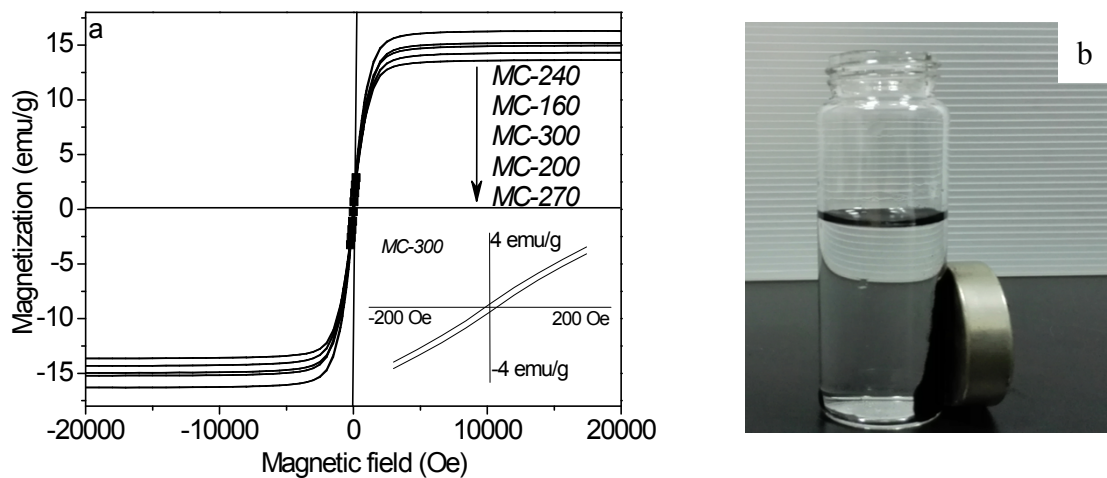


Fig. S6. (a) Hysteresis loop of the as-prepared magnetic carbon composites under 300 K (inset shows the hysteresis loop of MC-300 sample at  $\pm 200$  Oe) and (b) photo of magneto separation for the as-prepared magnetic carbon composite (MC-270).

Table S2. Ash and Fe<sub>2</sub>O<sub>3</sub> contents, magnetic property and acid resistance for different hydrochar-derived magnetic carbon composite

sample	ash (%)	Fe <sub>2</sub> O <sub>3</sub> (%)	<i>Ms</i> (emu/g) <sup>a</sup>	leaching (mg/L, pH 2) <sup>b</sup>	leaching (mg/L, pH 3) <sup>b</sup>
<i>MC-160</i>	18.1	15.9 ± 0.66	15.2	0.325 ± 0.003	0.0910 ± 0.001
<i>MC-200</i>	15.2	13.7 ± 0.35	14.3	0.419 ± 0.018	0.0685 ± 0.001
<i>MC-240</i>	17.4	15.3 ± 0.09	16.3	0.387 ± 0.006	0.131 ± 0.004
<i>MC-270</i>	13.2	11.4 ± 0.29	13.6	0.524 ± 0.001	0.153 ± 0.006
<i>MC-300</i>	14.2	12.4 ± 0.33	15.0	0.549 ± 0.004	0.149 ± 0.002

<sup>a</sup> *Ms* is saturation magnetization determined at room temperature.

<sup>b</sup> Fe leaching concentration determined at 2000 mg/L magnetic carbon composite with 24 h contact time at room temperature.

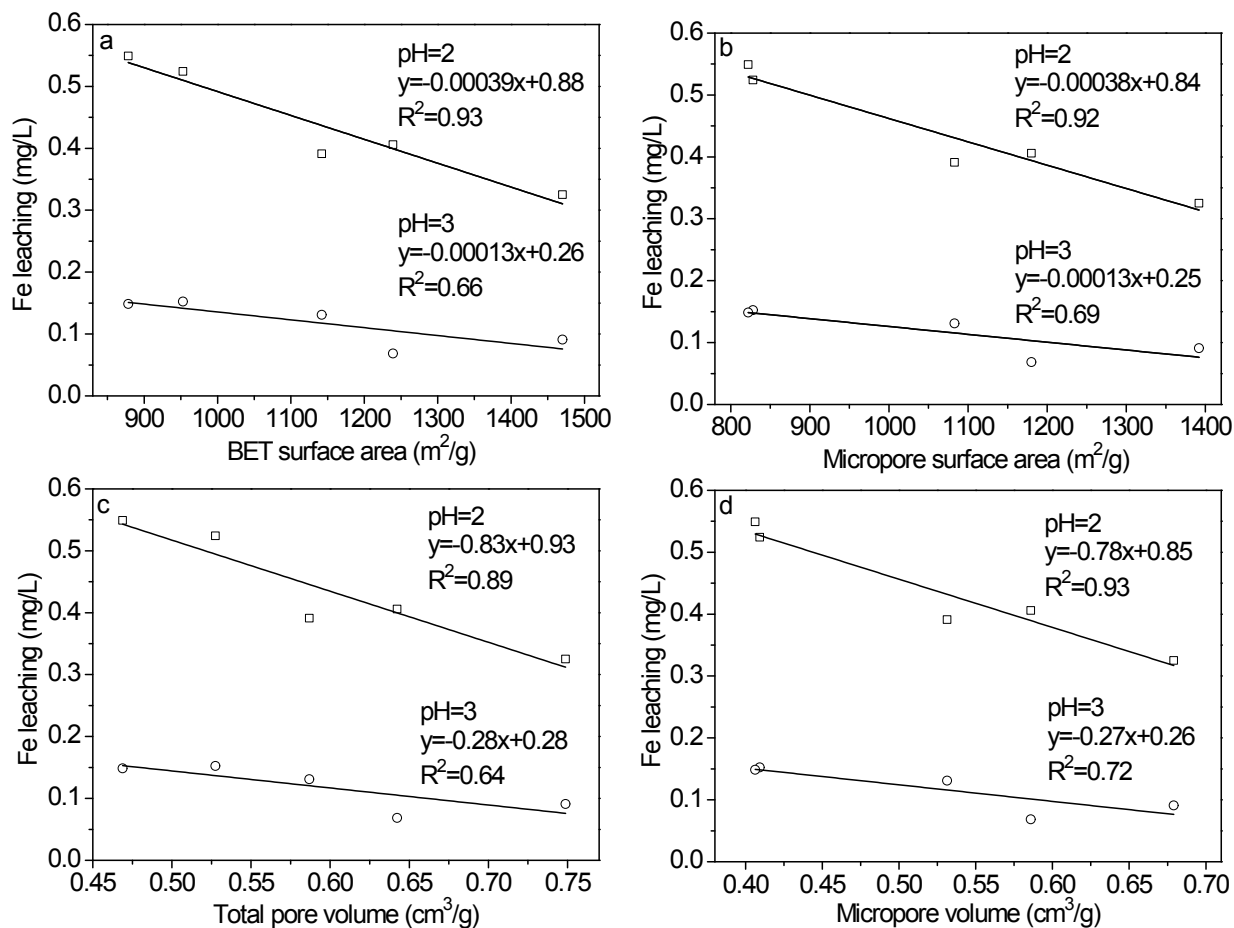


Fig. S7. Correlations between the Fe leaching concentration and the porosity of magnetic carbon composites: BET surface area (a), micropore surface area (b), total pore volume (c) and micropore volume (d).

Text S2

Adsorption kinetics is the most important characteristic in the representation of pollutants' uptake rates and adsorption efficiency.<sup>2, 3</sup> As shown in Fig. S8a, the adsorption reaction equilibrium was reached quickly, due to abundant adsorption sites for the ROX molecules. This is important for highly efficient removal of pollutants in the practical application of as-prepared magnetic carbon composites.

The pseudo-second-order kinetics equation was used to discuss the adsorption characteristics of ROX:

$$\frac{t}{q_t} = \frac{1}{k_2 q_e^2} + \frac{t}{q_e}$$

where  $t$  is the adsorption time,  $q_t$  (mg/g) is the ROX uptake at time  $t$ ,  $q_e$  (mg/g) is the ROX uptake at equilibrium, and  $k_2$  (g/mg·min) is the rate constant of pseudo-second-order adsorption.

As shown in Table 3, the correlation coefficient was 0.99 for all resultant magnetic carbon composites, and the pseudo-second-order kinetics equation exhibited a good fit for ROX adsorption, as further confirmed by Fig. S8b.

The changes in ROX adsorption capacity as a function of ROX concentration in the solution at equilibrium are shown in Fig. S9a. The Langmuir model was used to fit the adsorption data:

$$\frac{C_e}{q_e} = \frac{1}{b q_m} + \frac{C_e}{q_m}$$

where  $C_e$  (mg/L) is the equilibrium concentration of the ROX in the solution,  $q_m$  (mg/g) is the maximum adsorption capacity, and  $b$  (L/mg) is the Langmuir constant.

The linear forms of the Langmuir equation for the adsorption data were shown in Fig. S9b. As shown in Table 3 a high regression coefficient (0.99) for all cases revealed that Langmuir equation was well fitted to the adsorption of ROX. In addition, the as-prepared magnetic carbon composites exhibited a large adsorption capacity for ROX removal, indicating that this material can be an excellent candidate for the ROX removal.

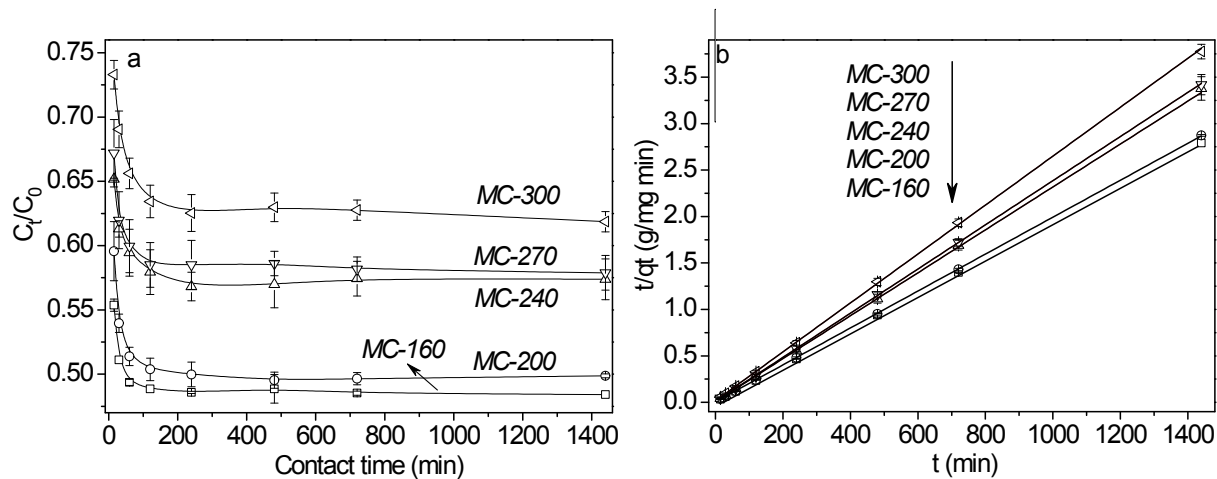


Fig. S8. (a) Adsorption of ROX onto as-prepared magnetic carbon composites as a function of time (ROX initial concentration: 400 mg/L). (b) Pseudo-second-order kinetics for ROX adsorption onto the as-prepared magnetic carbon composite: markers are experimental data and lines are the data predicated by the pseudo-second-order kinetics model.

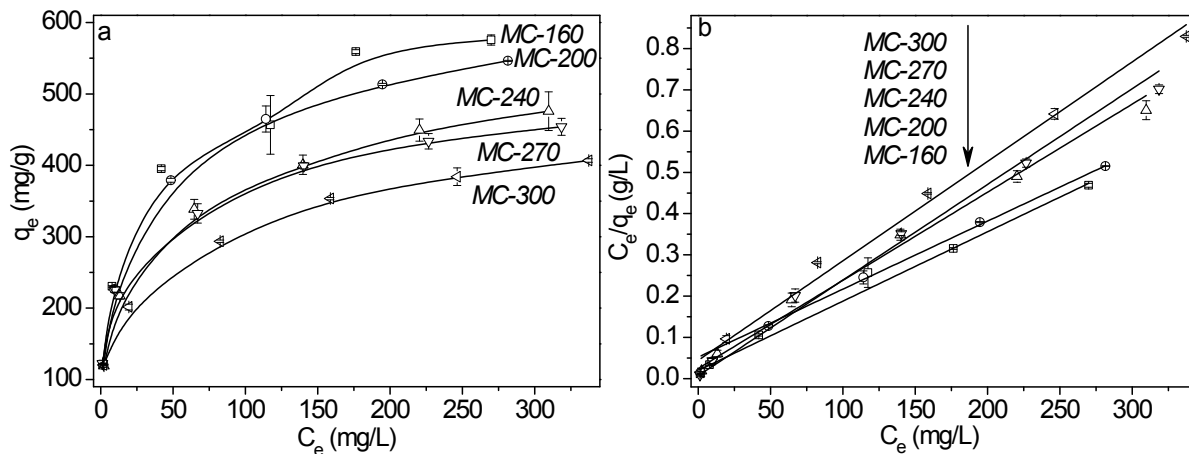


Fig. S9. (a) Adsorption isotherms of ROX onto as-prepared magnetic carbon composites. (b) Linear Langmuir equation for ROX adsorption onto as-prepared magnetic carbon composites: markers are experimental data and lines are the data predicated by the Langmuir model.

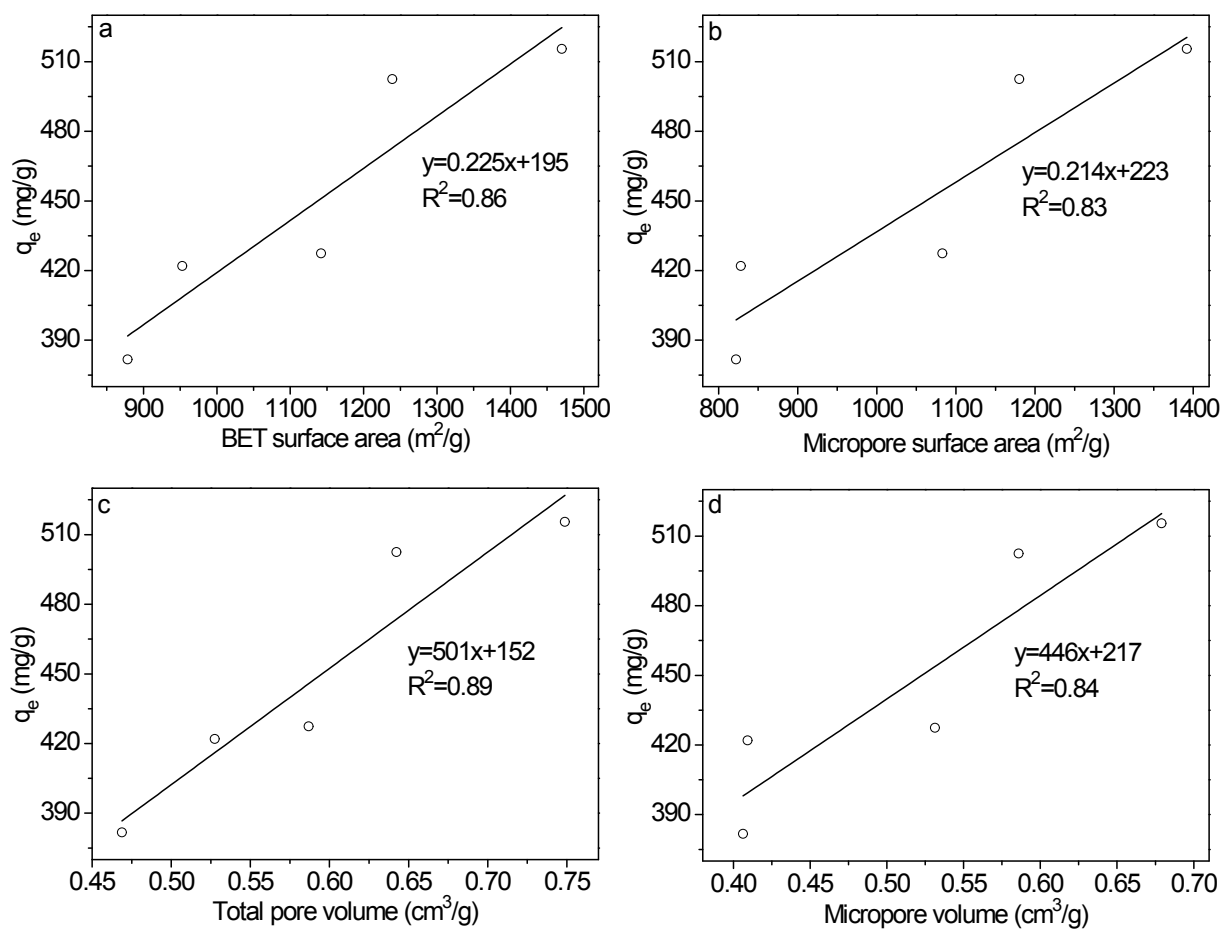


Fig. S10. Correlations between adsorption uptake at equilibrium ( $q_e$ , obtained from the pseudo-second-order kinetics equation at an initial ROX concentration of 400 mg/L) and porosity of magnetic carbon composites: BET surface area (a), micropore surface area (b), total pore volume (c) and micropore volume (d).

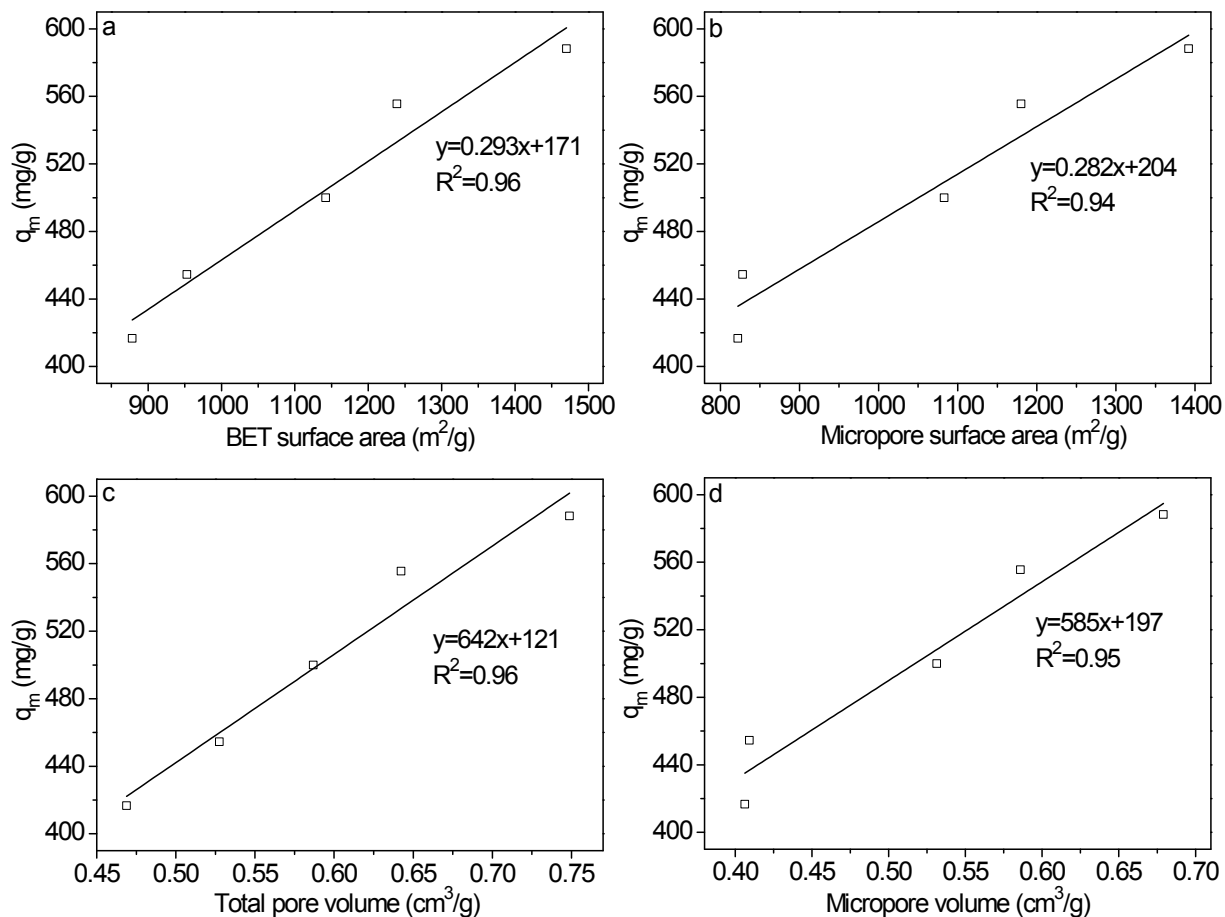


Fig. S11. Correlations between the maximum adsorption capacity ( $q_m$ , obtained from the Langmuir equation) and the porosity of magnetic carbon composites: BET surface area (a), micropore surface area (b), total pore volume (c) and micropore volume (d).

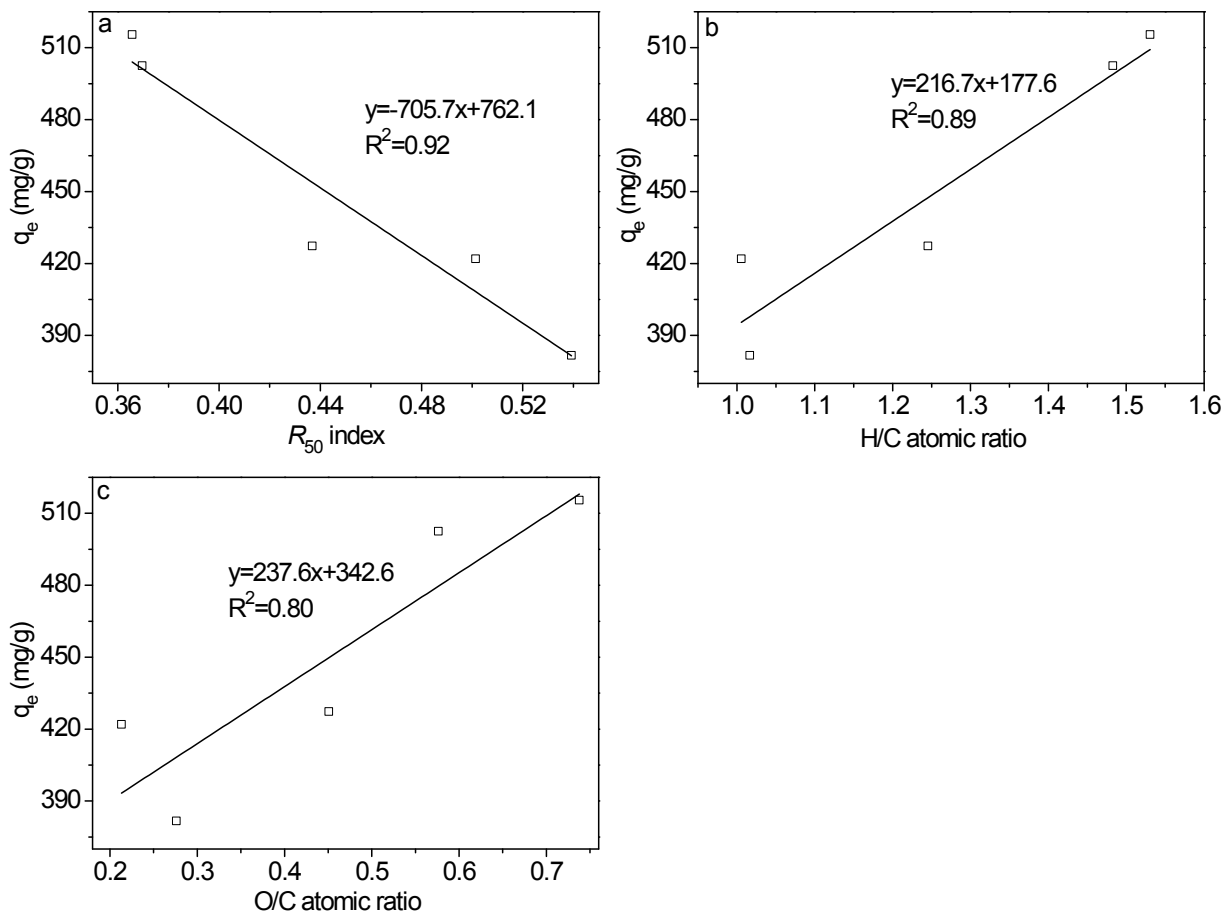


Fig. S12. Correlations between adsorption uptake at equilibrium ( $q_e$ , obtained from the pseudo-second-order kinetics equation at an initial ROX concentration of 400 mg/L) and properties of hydrochar:  $R_{50}$  index (a), H/C (b) and O/C (c) atomic ratios.

## References

- 1 O. R. Harvey, L.-J. Kuo, A. R. Zimmerman, P. Louchouart, J. E. Amonette and B. E. Herbert, *Environ. Sci. Technol.*, 2012, **46**, 1415-1421.
- 2 J. Hu, Z. Tong, Z. Hu, G. Chen and T. Chen, *J. Colloid Interf. Sci.*, 2012, **377**, 355-361.
- 3 J.X. Fan, Y.J. Wang, X.D. Cui and D.M. Zhou, *J. Soils Sediments*, 2013, **13**, 344-353.